Journal of Biomechanics 85 (2019) 50–58

Contents lists available at ScienceDirect

Journal of Biomechanics

journal homepage: www.elsevier.com/locate/jbiomech
www.JBiomech.com

Ankle intrinsic stiffness changes with postural sway

Pouya Amiri *, Robert E. Kearney

Department of Biomedical Engineering, McGill University, Montreal, Canada

ARTICLE INFO

Article history:
Accepted 3 January 2019

Keywords:
Ankle stiffness
Stance control
Postural sway
Intrinsic stiffness
Perturbed standing

ABSTRACT

In standing, the human body is inherently unstable and its stabilization requires constant regulation of ankle torque, generated by a combination of ankle intrinsic properties, peripheral reflexes, and central contributions. Ankle intrinsic stiffness, which quantifies the joint intrinsic properties, has been usually assumed constant in standing; however, there is strong evidence that it is highly dependent on the joint torque, which changes significantly with sway in stance. In this study, we examined how ankle intrinsic stiffness changes with postural sway during standing. Ten subjects stood on a standing apparatus, while subjected to pulse perturbations of ankle position. The mean torque of a short period before the start of each pulse was used as a measure of background torque. Responses with similar background torques were grouped together and used to estimate the parameters of an intrinsic stiffness model. Stiffness estimates were normalized to the critical stiffness and the background torque was transformed to the center of pressure location. We found that in most subjects, the normalized stiffness increased linearly with the movement of center of pressure towards the toes, with an average slope of 2.11 ± 0.80 1/m·rad. This modulation of ankle intrinsic stiffness seems functionally appropriate, since the intrinsic stiffness increases quickly, as the center of pressure moves toward the toes and the limits of stability. These large changes of ankle intrinsic stiffness with postural sway must be incorporated in any model of stance control.

1. Introduction

During stance, the human body acts as an unstable inverted pendulum that is subject to internal and external perturbations. Consequently, ankle torque must be modulated continuously to maintain stability (Loram et al., 2007). Ankle torque has two components. The first is intrinsic torque, generated by ankle intrinsic stiffness, which is the joint mechanical resistance to its movement with no intervention from the nervous system, generated by viscoelastic properties of the joint, active muscle fibers, and inertial properties of the limbs (Loram et al., 2007). The second is active torque, generated by changes in muscle activations, resulting from spinal reflexes and descending motor commands from brain. It is difficult to determine ankle intrinsic stiffness in functional tasks, such as standing, since the intrinsic and active torque appear together and cannot be separated easily. One method to quantify ankle intrinsic stiffness is to apply pulse perturbations of ankle position that generates an instantaneous intrinsic torque, followed by a delayed active torque response. The relationship between the joint angle and intrinsic torque defines the joint intrinsic stiffness and has been generally modelled as a mass-spring-damper (Loram and Lakie, 2002; Casadio et al., 2005).

Ankle intrinsic stiffness has been demonstrated to change dramatically with joint background torque (Mirbagheri et al., 2000; Golkar et al., 2017) and joint mean position (Mirbagheri et al., 2000; Sobhani Tehrani et al., 2017) in supine experiments. In standing ankle torque and angle change continuously with sway, therefore, it is likely that ankle intrinsic stiffness changes with sway. Despite this, some previous studies of standing have assumed that ankle intrinsic stiffness is constant in standing (Peterka, 2002; Casadio et al., 2005); Others examined the modulation of the stiffness with sway but found no consistent relation (Loram and Lakie, 2002). Recently Sakanaka et al. (2016) showed that the elastic component of ankle intrinsic stiffness increased with ankle torque in standing, when the body sway was artificially increased by continuous rotation of base of support. Consequently, we felt it important to determine the extent to which ankle intrinsic stiffness changes with sway in normal standing. To do so, we first developed a parametric model that captures the dynamics of ankle intrinsic stiffness during stance accurately. Then, we used this model to characterize how the stiffness changes with postural sway.

* Corresponding author at: Department of Biomedical Engineering, McGill University, Duff Medical Building, 3775 University Street, Room 306, Montreal, QC H3A 2B4, Canada.
E-mail address: pouya.amiri@mail.mcgill.ca (P. Amiri).

https://doi.org/10.1016/j.jbiomech.2019.01.009
0021-9290/

2. Methods

2.1. Participants

Ten subjects (6 male), aged between 18 and 40 years, with no history of neuromuscular disease were examined. Table 1 presents their anthropomorphic data. Subjects gave prior written consent to the experimental procedures, which had been approved by the McGill University's Research Ethics Board.

Table 1
Anthropometric data of the subjects (STD = standard deviation). For gender, M stands for male and F stands for female.

Subject number	Gender (M/F)	Age (years)	Height (m)	Mass (Kg)
1	F	31	1.65	57.0
2	M	27	1.68	64.5
3	M	25	1.75	93.7
4	M	23	1.67	67.0
5	M	29	1.77	68.6
6	M	23	1.72	72.0
7	M	27	1.82	79.7
8	F	25	1.76	67.1
9	F	24	1.59	60.1
10	F	30	1.52	56.0
Average ± STD	–	26.4 ± 2.9	1.69 ± 0.09	68.6 ± 11.3

2.2. Standing apparatus

Fig. 1A illustrates the experimental apparatus, which comprised two pedals, driven by servo-controlled, electro-hydraulic rotary actuators, capable of applying independent, bilateral angular position perturbations (Forster et al., 2003). Subjects stood with a foot on each pedal and their ankle axis of rotation aligned with that of the actuator. High performance rotary potentiometers (Maurey Instruments 112-P19) measured foot angle (θ_F), the pedal angle with respect to the horizontal (Fig. 1C). Each pedal was equipped with four load cells (The Omega™ LC302-100) that measured the vertical forces, used to compute ankle torque and the center of pressure (COP) position (Fig. 1B). Shank angles were measured using laser range finders as described in (Amiri et al., 2016). Fig. 1C shows the ankle angle, θ_A, the angle between the foot and the shank, given by:

$$\theta_A = \theta_F - \theta_S \quad (1)$$

where θ_S is the angle of the shank with respect to the vertical. By convention, dorsiflexing ankle angles and torques were taken as positive; a right angle between the foot and shank was taken as the zero ankle angle.

Body angle (θ_B) was determined by dividing the displacement of the mid-point between left and right posterior superior iliac spines, measured using another laser range finder (1302-200 Micro-epsilon, Fig. 1D), by the vertical distance between the laser and the ankle axis of rotation.

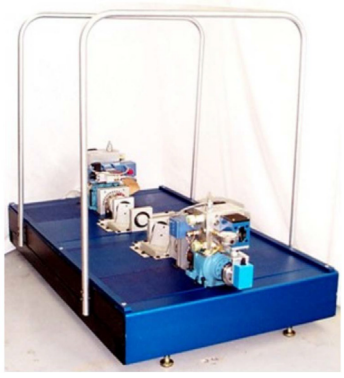

(A)

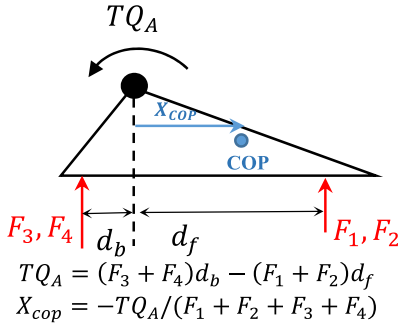

(B)

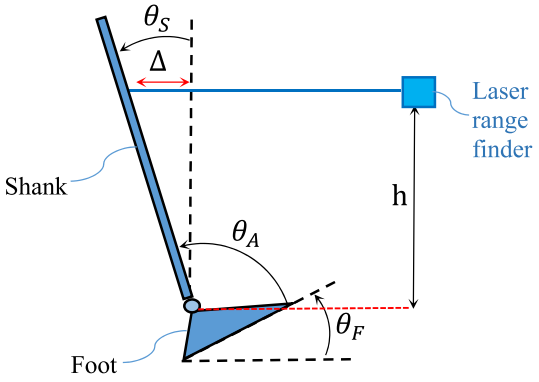

(C)

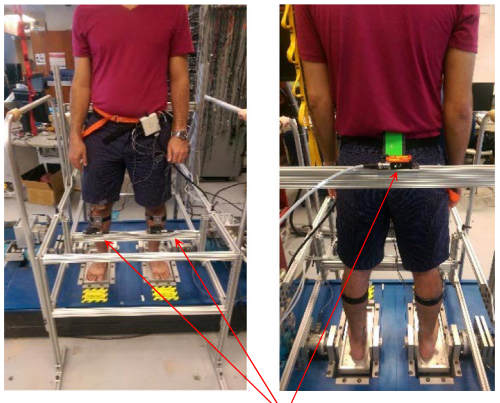

(D)

Range finders

Fig. 1. (A) Experimental apparatus, (B) Schematic of the forces, measured by the load cells and the equation to calculate ankle torque and COP location; (C) The shank angle (θ_S) was estimated by measuring its linear discplacement Δ and dividing it by the range finder height, h, above the ankle axis of rotation; foot angle (θ_F) was measured by the actuator potentiometer; ankle angle (θ_A) was obtained using Eq. (3); (D) The laser range finders used to measure shank and body movements.

2.3. EMG

Surface EMGs were measured from the major muscles about the ankle joint: the tibialis anterior (TA), and the three triceps surae (TS) muscles: the medial (MG) and lateral (LG) gastrocnemius, and soleus. Single differential Delsys electrodes with an inter-electrode distance of 1 cm were placed on the muscles, according to the Seniam guidelines (http://www.seniam.org/). EMGs were amplified with a gain of 1000 and filtered with a bandwidth of 20–2000 Hz.

2.4. Experiments

Subjects stood comfortably on the apparatus, looking forward, with their hands at their sides, and the mean foot angles set to 0 degree (Fig. 1D). First, a 60-second quiet standing trial (no perturbations) was performed for each subject. Then, the actuators applied uncorrelated, random position perturbations to both ankles simultaneously. Perturbations were pseudo random binary sequences (PRBS), where the actuator input switched between two values (peak-to-peak amplitude of 0.02 rad) at random multiples of 200 ms (Fig. 2A). The perturbations were not intended to emulate any real world situation but rather to measure the intrinsic stiffness while minimizing postural disturbances. We chose to use low amplitude perturbations with independent, random time courses to each ankle, since these evoke smaller postural disturbances than coherent perturbations to both ankles (Vlutters et al., 2015). Three two-minute trials, each with a different realization of the PRBS perturbation were acquired for each subject. Trials were separated by two minute rest periods to avoid fatigue.

2.5. Data acquisition

All signals were anti-alias filtered at 486.3 Hz and sampled at 1 KHz with 24-bit dynamic resolution. All sampled signals were low pass filtered at 50 Hz by a zero-phase shift 10th order Butterworth filter. Derivatives of the torques and angles were estimated using a digital differentiator (Westwick and Kearney, 2004).

2.6. Postural activity

Postural activity was quantified in terms of the mean and standard deviation of the body angle and rectified EMG. For the perturbed trials, the postural component of the EMG was estimated by eliminating the synchronous burst of reflex activity from the EMG record as described in Golkar et al. (2017).

2.7. Data segmentation and grouping

Ankle torque changed significantly throughout trials, due to postural sway as Fig. 2G shows. Such changes significantly change intrinsic stiffness (Mirbagheri et al., 2000; Golkar et al., 2017).

Fig. 2A shows that the PRBS position perturbation consisted of a sequence of pulse perturbations in alternating directions. Therefore, to account for changes in the ankle torque, we analyzed each pulse separately by finding local extrema of the foot velocity, and extracting signals for 50 ms before and 40 ms after the displacement. The right hand column of Fig. 2 shows a typical pulse response.

For analysis, we divided the responses into the two segments, shown in Fig. 2:

1. Pre-response segment: started 50 ms before the peak velocity and lasted for 25 ms. Foot position remained constant during this segment, so it defined the state of the ankle prior to the perturbation.
2. Intrinsic response segment: lasted from the end of the pre-response segment until 40 ms after the peak velocity. The reflex torques was substantial in some trials. However, our analysis

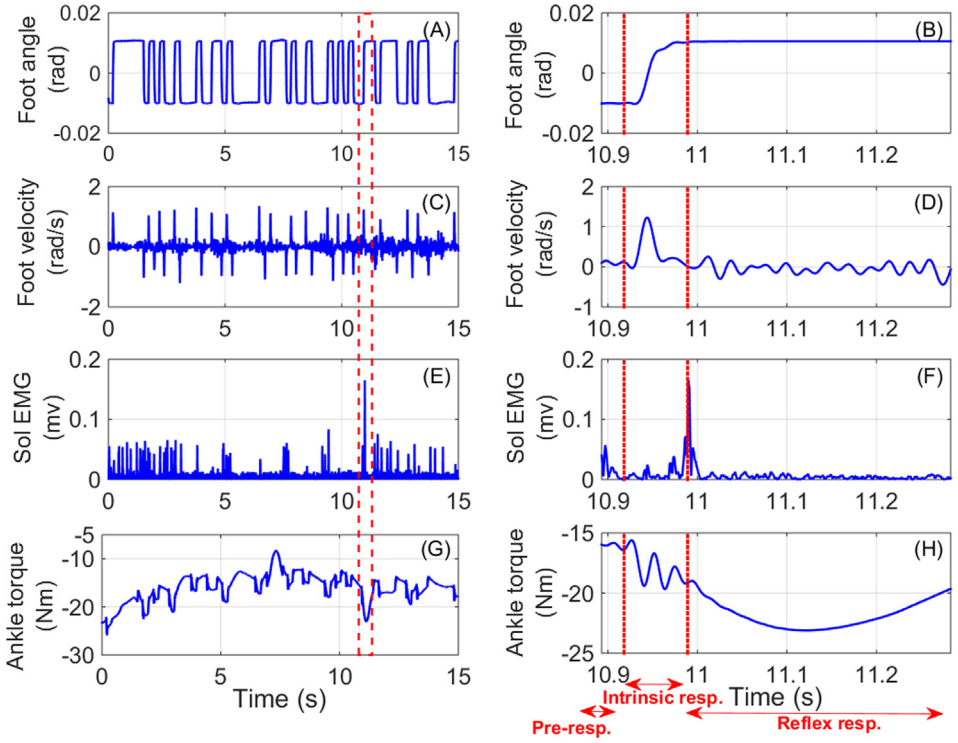

Fig. 2. Typical experimental trial. Left column shows 15 s of a typical trial, (A) Foot angle, (C) Foot velocity, (E) Soleus EMG, and (G) Ankle torque; The right column shows an individual pulse, encompassed by the red dashed box in the left column, on an expanded time scale: (B) Foot angle, (D) Foot velocity, (F) Soleus EMG, and (H) Ankle torque. The vertical dotted lines separate the response into the pre-response (0–25 ms), intrinsic response (26–90 ms), and reflex response (91–390 ms); positive torque and angles correspond to dorsiflexion. (For interpretation of the references to color in this figure legend, the reader is referred to the web version of this article.)

only considered data from the intrinsic response segment before any reflex torque could be generated. Consequently, we are confident that our estimates of the intrinsic stiffness were not affected by reflex torques.

To eliminate possible long lasting interactions between pulses, only pulses occurring more than 400 ms after a previous pulse were analyzed.

We also computed descriptive statistics for each pre-response including the mean torque (as a measure of background torque), the sum of mean rectified EMG of TS muscles, and TA muscle. Subsequently, intrinsic torque responses to pulse perturbations with similar background torques were grouped together, in 3 Nm bins, and used to estimate stiffness.

2.8. Intrinsic stiffness estimation

Due to the sluggish body dynamics, the perturbations should not evoke any significant shank movements during the intrinsic segment. Consequently, we modelled the stiffness as a function of foot angle only. Intrinsic stiffness has often been described using a mass-spring-damper (IBK) model (Loram et al., 2007; Amiri and Kearney, 2017):

$$\frac{\Delta TQ_I}{\Delta\theta_F} = (I_F + I_P)s^2 + Bs + K \tag{2}$$

where ΔTQ_I is the change in the ankle intrinsic torque, $\Delta\theta_F$ is the change in the foot angle, and I_F and I_P are the foot and pedal inertias.

However, recent evidence indicates that an *extended intrinsic model* (EIM), comprising a second order system with three zeros describes ankle intrinsic stiffness better (Sobhani Tehrani et al., 2017):

$$\frac{\Delta TQ_I}{\Delta\theta_F} = \frac{n_3s^3 + n_2s^2 + n_1s + K_{EIM}}{d_2s^2 + d_1s + 1} \tag{3}$$

Therefore, we compared the performance of the EIM and IBK model in standing. Parameters of each model were estimated using the regression formulation:

$$\Delta\boldsymbol{TQ_I} = \boldsymbol{X_{model}\theta_{model}} \tag{4}$$

where $\Delta\boldsymbol{TQ_I} = [\cdots \quad \Delta TQ_I(k) \quad \cdots]^T, k = 1,\ldots,N$ (N is the number of samples). For the IBK model the regression matrix $\boldsymbol{X_{model}}$ in (4) was:

$$\boldsymbol{X_{IBK}} = \begin{bmatrix} \vdots & \vdots & \vdots \\ \ddot{\theta}_F(k) & \dot{\theta}_F(k) & \Delta\theta_F(k) \\ \vdots & \vdots & \vdots \end{bmatrix}, \boldsymbol{\theta_{IBK}} = \begin{bmatrix} I \\ B \\ K \end{bmatrix} \tag{5}$$

and for the EIM was:

$$\boldsymbol{X_{EIM}} \begin{bmatrix} \vdots & \vdots & \vdots & \vdots & \vdots & \vdots \\ \dddot{\theta}_F(k) & \ddot{\theta}_F(k) & \dot{\theta}_F(k) & \Delta\theta_F(k) & \dot{TQ}_I(k) & \ddot{TQ}_I(k) \\ \vdots & \vdots & \vdots & \vdots & \vdots & \vdots \end{bmatrix}, \boldsymbol{\theta_{EIM}} = \begin{bmatrix} n_3 \\ n_2 \\ n_1 \\ n_0 \\ d_2 \\ d_1 \end{bmatrix} \tag{6}$$

Model parameters were estimated using the standard least squares solution:

$$\boldsymbol{\theta_{model}} = \left(\boldsymbol{X_{model}^T X_{model}}\right)^{-1} \boldsymbol{X_{model}^T \Delta TQ_I} \tag{7}$$

The estimated parameters were used to predict the intrinsic torque ($\widehat{\Delta TQ_I}$). Model performance was evaluated in terms of percentage variance accounted for (VAF):

$$VAF = 100\left(1 - \sum_{k=1}^{N}\left(\frac{\Delta TQ_I(k) - \widehat{\Delta TQ_I}(k))^2}{\sum_{k=1}^{N}\Delta TQ_I^2(k)}\right)\right) \tag{8}$$

Model performance was also evaluated in terms to the minimum description length (MDL) criterion, which balances the goodness of fit and the number of model parameters:

$$MDL(M) = \left(1 + \frac{Mlog(N)}{N}\right)\sum_{k=1}^{N}\left(\Delta TQ_I(k) - \widehat{\Delta TQ_I}(k,M)\right)^2 \tag{9}$$

where M is the number of model parameters (M = 3 for IBK model and M = 6 for EIM).

Given the low frequencies associated with postural control (van der Kooij et al., 2005), the low frequency stiffness is of primary interest. For the IBK model, this is equal to K, whereas, for the EIM, it is equal to K_{EIM}. Values of K and K_{EIM} were normalized to the subjects' critical stiffness, the minimum intrinsic stiffness required to maintain upright posture (Casadio et al., 2005), given by:

$$K_{cr} = mgh_{com} \tag{10}$$

where m is the subject's mass, g is gravitational acceleration, and h_{com} is the height of the body's center of mass above ankle axis of rotation, derived from anthropometric data (NASA, 1995).

3. Results

3.1. Quiet vs perturbed standing

The peak-to-peak amplitude of the perturbations was 0.02 rad; this was smaller than the range of the body angle in quiet standing, whose minimum was 0.025 rad (subject 1) and maximum was 0.041 rad (subject 3).

Mean body angle was similar (p = 0.965), but the RMS value of the angle was significantly greater in the perturbed (0.0 l7 ± 0.006 rad) than unperturbed trials (0.006 ± 0.002 rad). LG and soleus EMG remained unchanged, but MG activity increased more than 50% in perturbed trials; the ratio of perturbed/unperturbed MG RMS EMG was 1.51 ± 0.74 for the left and 1.61 ± 0.81 for the right side.

TA was silent in all subjects in unperturbed trials and in 8/10 subjects in perturbed trails. For these 8 subjects, the ratio of TA RMS activity in perturbed trials to its baseline activity in unperturbed trials was 1.13 ± 0.33 for the left and 1.33 ± 0.53 for the right side. In the two remaining subjects, the TA ratios of the left and right ankles were 9.1 and 11.2 (subject 2), and 10.0 and 4.6 (subject 9), showing substantial TA activity was present in perturbed trials.

3.2. Shank movement in response to foot perturbation

Fig. 3 shows the position and torque records from the intrinsic segment of a typical response group in blue and their ensemble averages in red. Fig. 3A and B demonstrate that the foot angle traces were very repeatable. However, as Fig. 3C and D show, the shank angles behaved differently. First, the ensemble average was almost completely flat, indicating that, during the intrinsic segment, there was no consistent shank movement in response to the foot perturbation. Thus, shank displacements cannot contribute to the intrinsic torque. Second, the mean shank angle varied from perturbation to perturbation, presumably reflecting postural sway. Fig. 3E and F demonstrate that the torque responses were consistent in shape, although offset from one another, presumably because of differences in ankle position.

3.3. Intrinsic stiffness model

Fig. 4 shows typical position perturbations in dorsiflexing (Fig. 4A) and plantar-flexing (Fig. 4B) directions. Fig. 4C and D show the measured torques, and those predicted by IBK model, and the EIM. Only a single pulse perturbation is shown, but all the perturbations in the group were used to estimate stiffness. The EIM prediction with a VAF of 99.4% was more accurate than IBK model, whose VAF was 98.3%. Fig. 4E and F also shows that the EIM residual torques (RMS = 0.17 Nm) were smaller than the IBK residuals (RMS = 0.29 Nm). Furthermore, the EIM estimate of low frequency stiffness (128.8 Nm/rad) was lower than that of the IBK model (138.4 Nm/rad).

Table 2 summarizes the performance of the EIM and IBK model. Note that the data for S7R was discarded, since it was corrupted by a large, low frequency noise whose origin we could not determine. The EIM model always fits the data very well with a %VAF greater than 95%, which was always greater than that of the IBK model. In addition, the ratio of the MDL cost function of the IBK model to EIM was always greater than 1, indicating that increased %VAF did not result from the increased model complexity. Finally, the median of the ratio of K_{EIM} to K was less than 1, indicating that the K_{EIM} estimates were consistently lower than those of K.

3.4. Low frequency ankle intrinsic stiffness

This section examines the relation between normalized K_{EIM} (K^N_{EIM}) and COP position. These variables, which normalize K_{EIM} and torque for differences in subjects' height and weight, reduce the inter-subject variability and simplify inter-subject comparisons.

Fig. 5 shows K^N_{EIM} as a function of COP position. The small confidence intervals show the high sensitivity of the EIM for the low frequency stiffness. IBK model showed similar sensitivity. There were large COP movements in most subjects, associated with large changes in K^N_{EIM}. Left and right ankle stiffness followed similar patterns, increasing with COP displacement, although their ranges differed due to differences in COP displacement. In three subjects the left and right stiffness were similar while in the other subjects the right ankle stiffness was consistently lower than the left at equivalent COP values.

Table 3 summarizes the ratio of the maximum K_{EIM} to its minimum, ranges of $\bar{TQ}_A$, K^N_{EIM} and COP. The ratio of the maximum to minimum K_{EIM} was smallest for S7L (1.20) and largest for S6R (5.63). In addition, the range of COP displacement varied from 2.9 cm to 6.5 cm and the range of K^N_{EIM} varied from 3% to a maximum of 19%.

Table 3 also shows the regression results between K^N_{EIM} and COP, demonstrating that in most cases, K^N_{EIM} increased almost linearly with COP movement. In 15/19 cases, the coefficient of determination (COD) was greater than 0.639 and slopes were non-zero (P-value < 0.05). In one case (S1R), the stiffness appeared to saturate for large COPs. In the remaining cases (S2R, S9L, and S9R), there was no significant change in stiffness with COP.

To understand this, we examined how COP and background EMGs varied. Fig. 6A and C shows that for a typical subject, K^N_{EIM} and background TS EMG increased with COP, while the TA remained silent. In contrast, Fig. 6B and D shows that for S9L, K^N_{EIM} stayed almost constant; in this case, TA was active at low COP and decreased as COP increased, whereas TS activity increased. The same behavior was seen in S2R and S9R.

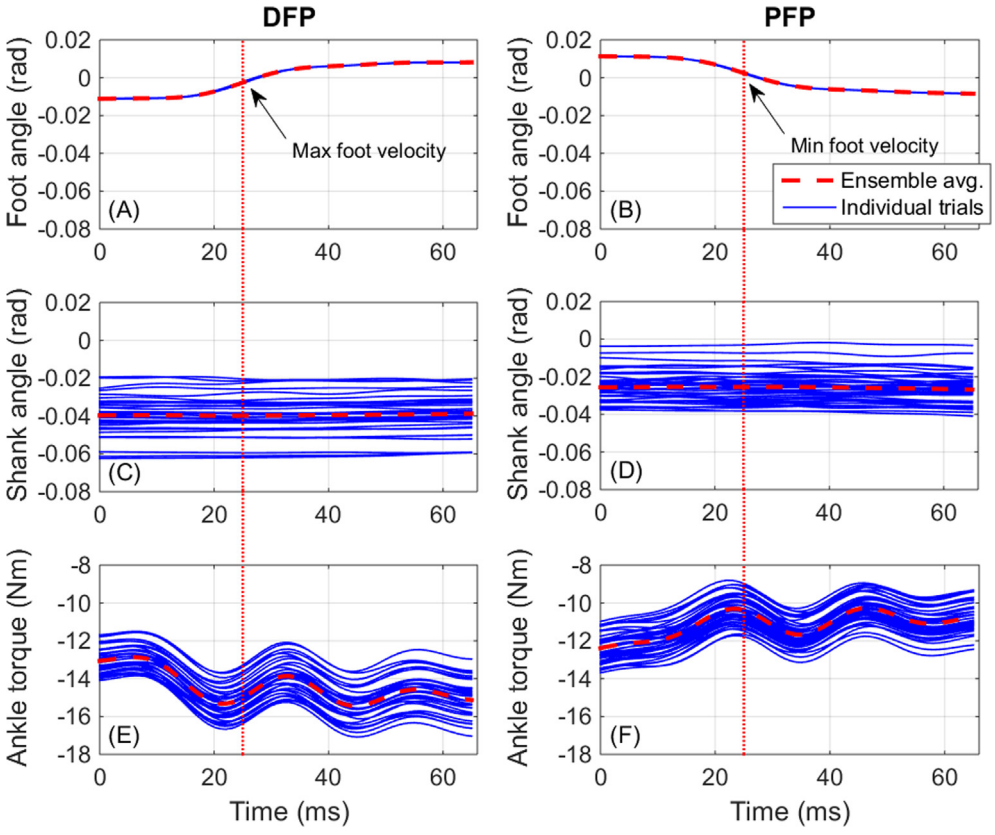

Fig. 3. Typical group of intrinsic responses to dorsiflexing (DFP, left column) and plantar-flexing pulses (PFP, right column). (A and B) Foot angle, (C and D) Shank angle, (E and F) Ankle torque. Individual responses are shown in blue and their ensemble averages in red. Background torque range is 11–14 Nm for subject 1's left ankle. (For interpretation of the references to color in this figure legend, the reader is referred to the web version of this article.)

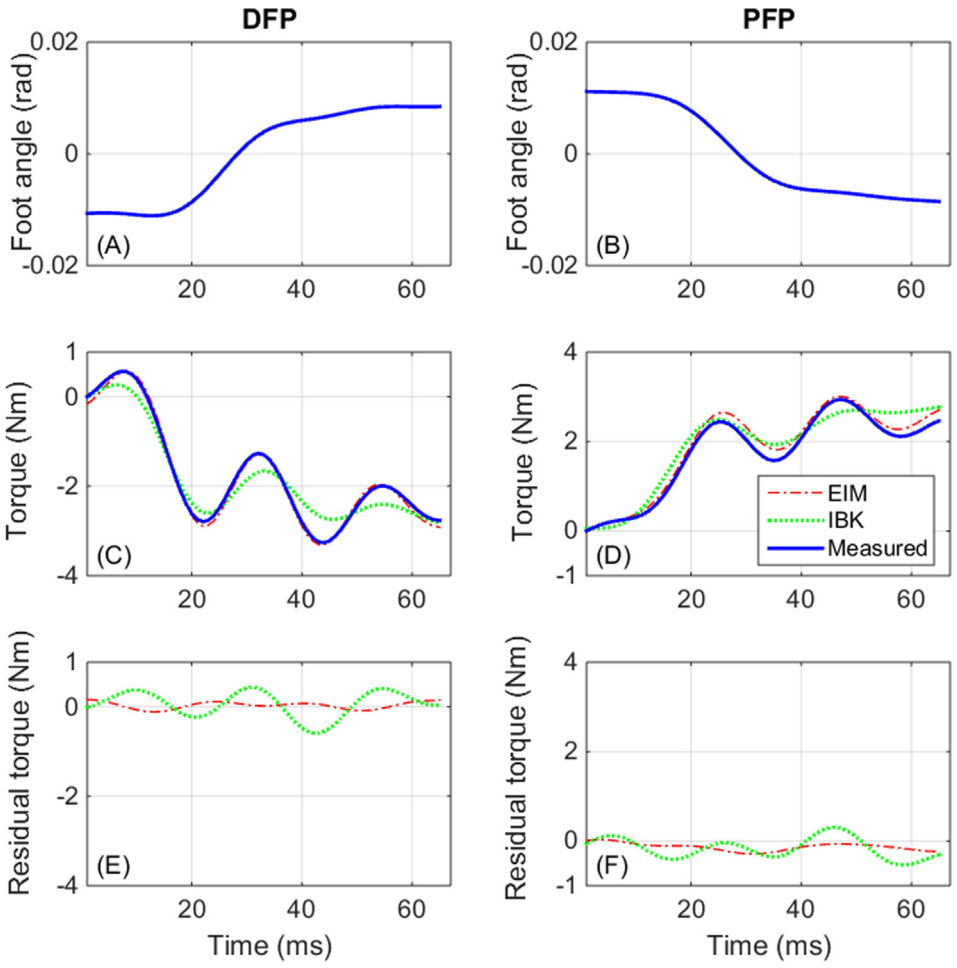

Fig. 4. Torques predicted by the IBK model and EIM for typical dorsiflexing (DFP) and plantarflexing (PFP) pulses. (A and B) Foot angle, (C and D) Experimental, IBK model, and EIM torques, (E and F) Residual torques for the IBK model and EIM. The results belong to Subject 1′s left ankle at background torque 22.5 Nm.

Table 2
EIM and IBK model performance for all subjects. Min and max stand for minimum and maximum. IQR shows the interquartile range.

	Left ankle				Right ankle			
	Min	Max	Median	IQR	Min	Max	Median	IQR
%VAF	96.6	99.7	98.9	1.0	95.2	99.4	98.6	1.5
$\%VAF_{EIM}$-VAF_{IBK}	0.8	5.7	1.8	1.4	2.6	26.2	6.0	3.4
MDL_{IBK}/MDL_{EIM}	1.60	4.75	2.30	0.72	1.70	9.47	3.35	2.13
K_{EIM}/K	0.78	0.91	0.93	0.03	0.75	1.13	0.90	0.09

4. Discussion

We showed that ankle intrinsic stiffness is not constant in standing, but changes significantly with postural sway; indeed in some subjects the intrinsic stiffness varied more than five-fold. These findings call into question the common assumption that ankle intrinsic stiffness is constant in stance (Loram and Lakie, 2002; Peterka, 2002; Casadio et al., 2005; Kiemel et al., 2008).

4.1. The intrinsic stiffness model

Ankle intrinsic stiffness has often been modelled as a mass-spring-damper system (Casadio et al., 2005; Loram et al., 2007; Amiri and Kearney, 2017). However, intrinsic dynamics may become more complex under certain operating conditions (Sobhani Tehrani et al., 2017). Our results showed that EIM is required to model the intrinsic stiffness during stance.

This conclusion is supported by the finding that the VAF of the EIM was higher than that of the IBK model. Moreover, this increase was not simply due to the added complexity, since, the MDL, which accounts for both the accuracy and complexity of a model, was always higher for the IBK model than the EIM. The stiffness estimates obtained with both the IBK and EIM models followed similar trends, but as Table 2 illustrates, the EIM estimates were consistently smaller than the IBK estimates. Sobhani Tehrani et al. (2017) demonstrated that fits with the EIM model yields more accurate estimates of the low frequency gain. Consequently, we believe the EIM results provide a better indication of the contribution of intrinsic stiffness to postural control

4.2. Intrinsic stiffness

Our results demonstrated that ankle intrinsic stiffness changes with postural sway during stance. More specifically, the low

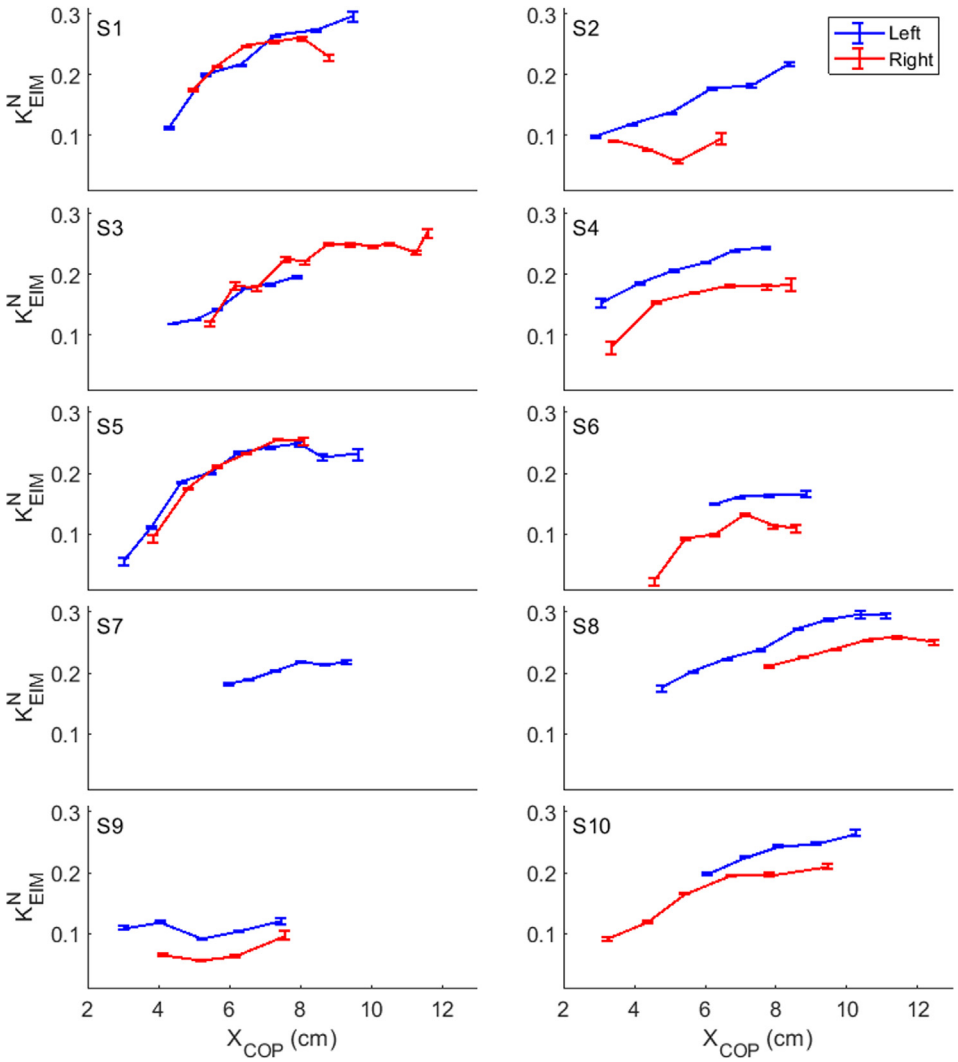

Fig. 5. Relation between normalized intrinsic stiffness and COP position. Each panel shows the left (blue) and right (red) stiffness for one subject; bars indicate the 95% confidence intervals of the stiffness values. Note that S7R was discarded. (For interpretation of the references to color in this figure legend, the reader is referred to the web version of this article.)

Table 3
Changes of K_{EIM} with COP for the left and right ankles of subjects. The ratio of maximum K^N_{EIM} (K^{max}_{EIM}) to minimum K^N_{EIM} (K^{min}_{EIM}) and the range (maximum-minimum) of the estimated parameters, including K^N_{EIM}, background torque ($\overline{TQ}_A$), and COP (X_{cop}); and the results of linear regressions analysis for the relation between K^N_{EIM} and X_{cop} for all subjects. P value is the probability of the slope being zero. The last column shows mean and standard deviation (std) of each parameter. To find the mean and standard deviation for slope, intercept, and R-squared, only the lines with a non-zero slope (i.e. with p-value < 0.05) were used.

Subject			1	2	3	4	5	6	7	8	9	10	mean ± std
Critical stiffness (Nm/rad)			471.6	548.1	832.9	563.2	601.6	617.4	721.5	590.3	478.8	432.0	585.7 ± 120.6
Left ankle	$K^{max}_{EIM}/K^{min}_{EIM}$		2.63	2.21	1.65	1.59	4.46	1.23	1.20	1.69	1.31	1.34	1.93 ± 1.00
	Range	K^N_{EIM}	0.18	0.12	0.08	0.09	0.19	0.03	0.04	0.12	0.03	0.07	0.10 ± 0.06
		$\overline{TQ}_A$(Nm)	18	18	18	18	27	15	18	24	15	15	19 ± 4
		X_{cop}(cm)	5.2	5.5	3.5	4.7	6.5	3.1	3.4	5.7	3.7	3.6	4.5 ± 1.2
	Linear regression	Slope (1/m·rad)	3.26	2.15	2.41	1.93	2.51	0.97	1.14	2.22	0.08	1.75	2.04 ± 0.70
		P value	0.004	0.000	0.001	0.000	0.005	0.036	0.006	0.000	0.875	0.006	–
		Intercept $\times 10^{-2}$ (1/rad)	0.00	3.46	1.00	10.23	3.84	9.24	11.80	9.10	10.53	11.53	6.69 ± 4.61
		R^2	0.897	0.977	0.957	0.968	0.695	0.816	0.879	0.961	0.001	0.942	0.899 ± 0.093
Right ankle	$K^{max}_{EIM}/K^{min}_{EIM}$		1.49	1.65	2.24	2.32	3.03	5.63	–	1.21	1.72	3.10	2.49 ± 1.35
	Range	K^N_{EIM}	0.09	0.04	0.15	0.11	0.18	0.11	–	0.05	0.04	0.14	0.10 ± 0.05
		$\overline{TQ}_A$(Nm)	18	12	33	18	18	18	–	18	12	18	18 ± 6
		X_{cop}(cm)	3.9	3.0	6.2	5.1	4.4	3.8	–	4.3	2.9	5.3	4.3 ± 1.1
	Linear regression	Slope (1/m·rad)	1.51	0.00	1.86	1.77	3.98	2.11	–	1.04	1.11	2.59	2.23 ± 1.00
		P value	0.084	0.999	0.000	0.033	0.002	0.047	–	0.013	0.186	0.010	–
		Intercept $\times 10^{-2}$ (1/rad)	12.68	8.02	6.00	5.04	0.00	0.00	–	14.80	0.00	2.28	4.69 ± 5.55
		R^2	0.475	0.000	0.764	0.719	0.935	0.639	–	0.822	0.662	0.840	0.787 ± 0.103

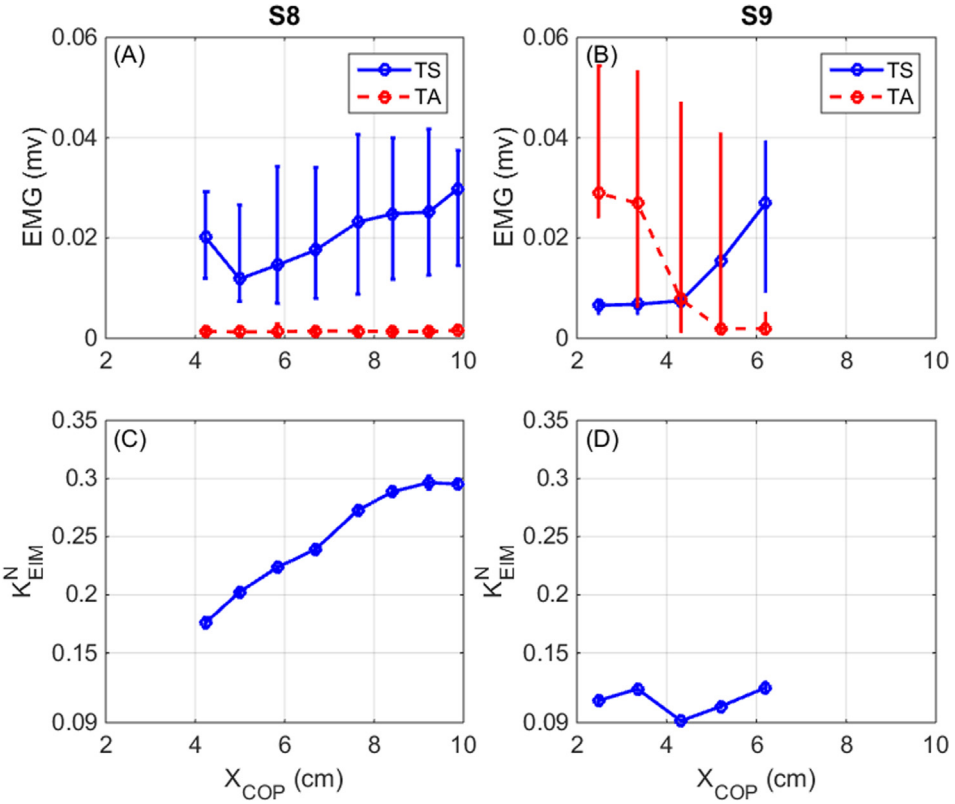

Fig. 6. The influence of ankle muscle activity on the joint stiffness of subject 8′s left ankle, (S8, left column) and subject 9′ left ankle (S9, right column); (A and B) the EMG activity of the TS and TA muscles, and (C and D) the corresponding joint stiffness. In (A and B) the bars show the min and max and the circle shows the median of the background EMG activity at each background torque. In the bottom row, K^N_{EIM} is shown with its 95% confidence interval.

frequency gain of intrinsic stiffness increases as the COP moves away from the ankle axis of rotation (Fig. 5). This relationship between the stiffness and joint torque has been reported in supine conditions (Mirbagheri et al., 2000; Golkar et al., 2017). However, many studies of stance have assumed ankle intrinsic stiffness to be constant (Peterka, 2002; Kiemel et al., 2008). Some tried to show the stiffness changes with ankle torque in standing but they failed and concluded the stiffness was a biomechanical constant (Loram and Lakie, 2002). One study recently demonstrated that ankle intrinsic stiffness varied with background torque when body sway was increased by slowly rotating the support surface (Sakanaka et al., 2016). The current work systematically investigated the modulation of ankle intrinsic stiffness with postural sway in standing.

In most subjects, the left and right ankles showed similar trends, whereby stiffness increased with COP displacement. Two differences in behavior were evident. First, in some subjects, the range of COP changes was different between the limbs, resulting in differences in the range of stiffness (e.g. subject 3). We do not believe these differences result from the application of perturbations, since differences in the range of left and right COP displacements during perturbed trials were similar to those during unperturbed trials. Secondly, in six subjects, the trends were similar but there was an offset, so that the stiffness of the right ankle was lower than that of the left ankle at all COPs. We do not believe this was the result of the perturbations either, since EMG activity increased by a similar amount in the left and right MG in comparison to unperturbed trials and there was no evidence of co-contraction in most cases. Consequently, we believe that these differences likely represent inherent differences in the passive joint stiffness (i.e. stiffness with no muscle activity).

An important question is the extent to which ankle intrinsic stiffness contributes to overall stance control. Normalized stiffness (K^N_{EIM}) provides a convenient measure of this. We estimated the minimum contribution of the stiffness for each subject as the sum of the lowest normalized stiffness values of the left and right ankles. Similarly, we estimated the maximum contribution as the sum of the maximum values of the two sides. Fig. 7 shows the range of combined stiffness values for each subject. Our estimates of the combined normalized stiffness of the two ankles ranged from a minimum of 14.7% (subject 5) to a maximum of 55.7% (subject 1). Other studies have reported higher values for the stiffness: Loram et al. 91% (Loram and Lakie, 2002), Casadio et al. 64% (Casadio et al., 2005), Sakanaka et al. 45–80% (Sakanaka et al., 2016), and Vlutters et al. 40–70% (Vlutters et al., 2015). These differences likely arise from differences in the perturbation amplitudes. Ankle intrinsic stiffness decreases as perturbation amplitude increases (Kearney and Hunter, 1982; Vlutters et al., 2015). The peak to peak amplitude of the perturbations in our study was 1.15° (0.02 rad), which was larger than that used in other studies (Loram 0.055°, Casadio 1°, Sakanaka < 0.6°, and Vlutters 0.29–4.6°).

Two other factors may also have contributed to the differences of low frequency stiffness estimates. First, other studies used an IBK model for the intrinsic stiffness, while we used the EIM, which yields lower values for the stiffness. Second, other studies obtained mean stiffness values by averaging torque responses to pulses, assuming that stiffness is constant. This approach masks the dependency of the stiffness on ankle torque. Despite the difference in the stiffness values, consistent with other studies (Loram and Lakie, 2002; Casadio et al., 2005; Kiemel et al., 2008; Vlutters et al., 2015), our results showed that although ankle intrinsic

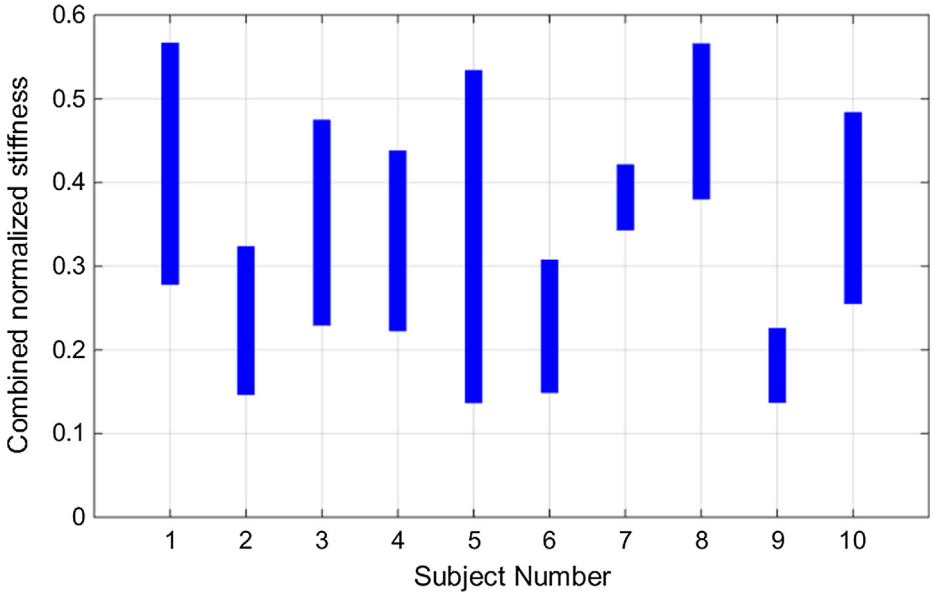

Fig. 7. Range of combined normalized stiffness (left minimum stiffness + right minimum stiffness to left maximum stiffness + right maximum stiffness) for all subjects.

stiffness is not sufficient for stance control, it is large enough to contribute significantly to stance control.

4.3. Functional significance of the modulation of ankle intrinsic stiffness in stance

We found that postural sway and MG activity increased when perturbations were applied, indicating that these made postural control more challenging. However, there was no change in mean body position and in all but two subjects only the plantar-flexors muscles were active, indicating that there was no major change in postural control strategy. Consequently, we believe that the results of our study are representative of changes to be expected in unperturbed standing.

The modulation of ankle intrinsic stiffness seems to be functionally appropriate for the control of stability in standing. Thus, when the COP is closer to the limits of stability and the body is more prone to fall, ankle intrinsic stiffness is higher. Therefore, the common assumption that the contribution of intrinsic stiffness to stance control is constant may ignore an important feature of postural control.

Acknowledgments

This paper was made possible by NPRP grant #6-463-2-189 from the Qatar National Research Fund (a member of Qatar Foundation) and MOP grant #81280 from the Canadian Institutes of Health Research (CIHR). The statements made herein are solely the responsibility of the authors.

Conflict of interest

The authors have no conflict of interest.

References

Amiri, P., Kearney, R.E., 2017. Ankle intrinsic stiffness is modulated by postural sway. Conf. Proc. IEEE Eng. Med. Biol. Soc. 2017, 70–73.

Amiri, P., MacLean, L.J., Kearney, R.E., 2016. Measurement of shank angle during stance using laser range finders. International Conference of the IEEE Engineering in Medicine and Biology.

Casadio, M., Morasso, P.G., Sanguineti, V., 2005. Direct measurement of ankle stiffness during quiet standing: implications for control modelling and clinical application. Gait Post. 21 (4), 410–424.

Forster, S.M., Wagner, R., Kearney, R.E., 2003. A bilateral electro-hydraulic actuator system to measure dynamic ankle joint stiffness during upright human stance. In: Proceedings of the 25th Annual International Conference of the IEEE Engineering in Medicine and Biology Society (IEEE Cat. No.03CH37439).

Golkar, M.A., Sobhani Tehrani, E., Kearney, R.E., 2017. Linear parameter varying identification of dynamic joint stiffness during time-varying voluntary contractions. Front. Comput. Neurosci. 11, 35 http://www.seniam.org/.

Kearney, R.E., Hunter, I.W., 1982. Dynamics of human ankle stiffness: variation with displacement amplitude. J. Biomech. 15 (10), 753–756.

Kiemel, T., Elahi, A.J., Jeka, J.J., 2008. Identification of the plant for upright stance in humans: multiple movement patterns from a single neural strategy. J. Neurophysiol. 100 (6), 3394–3406.

Loram, I.D., Maganaris, C.N., Lakie, M., 2007. The passive, human calf muscles in relation to standing: the non-linear decrease from short range to long range stiffness. J. Physiol. 584 (Pt 2), 661–675.

Loram, I.D, Lakie, M., 2002. Direct measurement of human ankle stiffness during quiet standing: the intrinsic mechanical stiffness is insufficient for stability. J. Physiol. 545 (Pt 3), 1041–1053.

Mirbagheri, M.M., Barbeau, H., Kearney, R.E., 2000. Intrinsic and reflex contributions to human ankle stiffness: variation with activation level and position. Exp. Brain Res. 135 (4), 423–436.

NASA, 1995. Anthropometry and Biomechanics. From <http://msis.jsc.nasa.gov/sections/section03.htm>.

Peterka, R.J., 2002. Sensorimotor integration in human postural control. J. Neurophysiol. 88 (3), 1097–1118.

Sakanaka, T.E., Lakie, M., Reynolds, R.F., 2016. Sway-dependent changes in standing ankle stiffness caused by muscle thixotropy. J. Physiol. 594 (3), 781–793.

Sobhani Tehrani, E., Jalaleddini, K., Kearney, R.E., 2017. Ankle joint intrinsic dynamics is more complex than a mass-spring-damper model. IEEE Trans. Neural Syst. Rehabil. Eng. 25 (9), 1568–1580.

van der Kooij, H., van Asseldonk, E., van der Helm, F.C., 2005. Comparison of different methods to identify and quantify balance control. J. Neurosci. Meth. 145 (1–2), 175–203.

Vlutters, M., Boonstra, T.A., Schouten, A.C., van der Kooij, H., 2015. Direct measurement of the intrinsic ankle stiffness during standing. J. Biomech. 48 (7), 1258–1263.

Westwick, D.T., Kearney, R.E., 2004. An object-oriented toolbox for linear and nonlinear system identification. Conf. Proc. IEEE Eng. Med. Biol. Soc. 1, 514–517.